Supporting Information

Enhanced and High-Purity Enrichment of Circulating Tumor Cells Based on Immunomagnetic Nanospheres

Xu-Yan Ma,[†,§] Ling-Ling Wu,[†,§] Lan Chen,[†] Yin-Hui Qin,[†] Jiao Hu,[†] Man Tang,[†]

Chun-Miao Xu,[†] Chu-bo Qi,[†,‡] Zhi-Ling Zhang,[†] Dai-Wen Pang[*,†]

[†] Key Laboratory of Analytical Chemistry for Biology and Medicine (Ministry of Education), College of Chemistry and Molecular Sciences, State Key Laboratory of Virology, The Institute for Advanced Studies, and Wuhan Institute of Biotechnology, Wuhan University, Wuhan 430072, P.R. China.

[‡] Hubei Cancer Hospital, Wuhan, 430079, P.R. China.

[§] Xu-Yan Ma and Ling-Ling Wu contributed equally to this work.

Corresponding Author

Email: dwpang@whu.edu.cn. Tel: 0086-27-68756759. Fax: 0086-27-68754067

Table of Contents for Supporting Information

The number of the effective binding sites on each IMN. To load sufficient number of antibodies on MNs, MNs were reacted with excessive antibodies, and the loading efficiency of antibody on the IMNs was not high theoretically. Hence, compared with the loading efficiency of antibody on the IMNs, we paid more attention to the number of the effective binding sites on each IMN. First, the IMNs (CD45) were mixed with FITC labeled IgG to fabricate IMNs-FITC-IgG, and the absorbance at 600 nm and fluorescence intensity of IMNs-FITC-IgG were measured. Then, the proportional relationship of absorbance at 600 nm versus MN concentration was measured to worked out the concentration of IMNs (CD45) (Figures S1A). In addition, in the presence of MNs at the same concentration with that of detected IMNs (CD45), the standard curve was got by recording the FITC labeled IMNs (CD45) at different concentration (Figures S1B). Based on these, the number of the effective binding sites on each IMN (CD45) could be calculated. The experiment was operated three times, and the number of the effective binding sites on each IMN (CD45) was evaluated to be about 100.

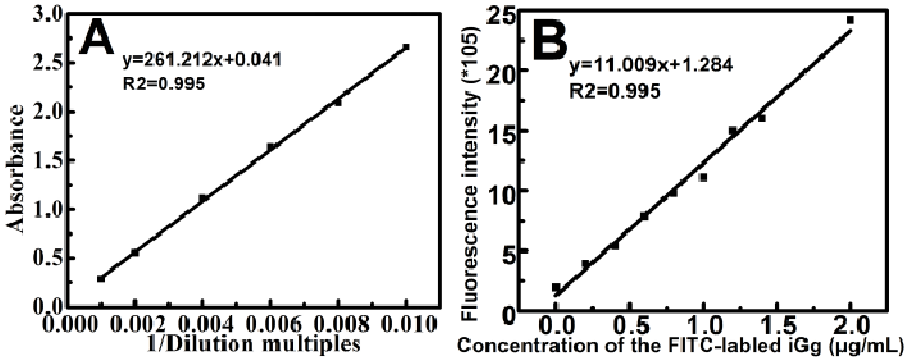

Figure S1. (A) Proportional relationship of absorbance at 600 nm versus MN concentration. (B) Standard curve of the FITC labeled IgG of different concentrations in the presence of MNs at the same concentration with that of IMNs (CD45).

The bioactivity of the antibodies modified on the IMNs. The stability of the IMNs is very important for immune capture and isolation, which is also what we concerned. We monitored the bioactivity of the antibodies modified on the IMNs for a long time. As shown in Figure S2A, the antibodies modified on the IMNs could react with Dylight 488-labele

goat anti-mouse IgG after 6 months' storage. Besides, IMNs could capture more than 90% of target cells even after 6 months' storage (Figures S2(B-C)). These results confirmed that antibodies modified on the IMNs preserved their biological activity for a long storage time.

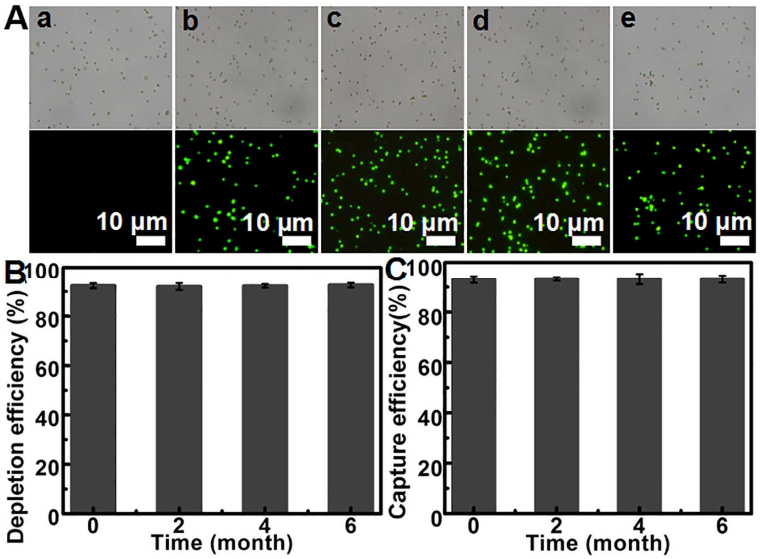

Figure S2. (A) Fluorescence microscopy images of MNs, IMNs (CD45) and IMNs (EpCAM & EGFR) newly-prepared (a-c) or after 6 months' storage (d-e) after treatment with Dylight 488-labeled goat anti-mouse IgG. (B) Depletion efficiency of IMNs (CD45) to Jurkat T cells with different storage time. (C) Capture efficiency of IMNs (EpCAM & EGFR) to tumor cells with different storage time.

Specificity of the binding between IMFNs and target cells. To demonstrate the specific binding between immunonanospheres and cells, immunomagnetic fluorescent nanospheres (IMFNs) modified with different antibodies were used to treat Jurkat T, MCF-7 and MDA-MB-231 cells respectively. After that, the cells were observed under an inverted fluorescence microscope, which was shown in Figure S3. It could be seen that IMFNs (CD45) successfully bound to Jurkat T cells surface, and no red fluorescence was observed on both MCF-7 and MDA-MB-231 cells (Figure S3A), while the IMFNs (EpCAM & EGFR) had the opposite result (Figure S3B), indicating that the immunonanospheres have

good specificity. The magnetic fluorescent nanospheres were also prepared with layer-by-layer assembly method (two layers of hydrophobic CdSe/ZnS quantum dots, and three layers of nano-γ-Fe_2O_3).

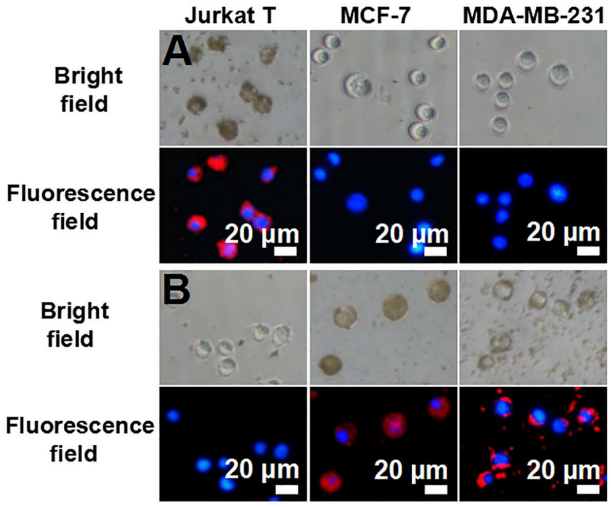

Figure S3. Microscopic images of Jurkat T, MCF-7 and MDA-MB-231 cells reacted with IMFNs (CD45) (A) and IMFNs (EpCAM & EGFR) (B). All these cells were Hoechst 33342-prestained.

Comparison of capture efficiency with IMNs (EpCAM & EGFR), IMNs (EpCAM) and IMNs (EGFR). To compare the enhanced capture efficiency of IMNs (EpCAM & EGFR) with these of IMNs (EpCAM) and IMNs (EGFR), the cocktail of 5 x 10^4 MCF-7 cells and 5 x 10^4 MDA-MB-231 cells was incubated with IMNs (EpCAM & EGFR), IMNs (EpCAM) and IMNs (EGFR) respectively. Then, separated with a magnetic scaffold, and the captured and uncaptured cells were observed under an inverted fluorescence microscope. (MCF-7 cells were Hoechst 33342-prestained and MDA-MB-231 cells were DiI-prestained) Figure S3 showed that IMNs (EpCAM) could capture EpCAM-positive MCF-7 cells (blue),

but hardly bind EpCAM-negative MDA-MB-231 cells (Red) (Figure S4A), IMNs (EGFR) could capture MDA-MB-231 cells (Red) but hardly bind MCF-7 cells (blue) (Figure S4B), while both MCF-7 cells and MDA-MB-231 cells were efficiently captured with IMNs (EpCAM & EGFR) (Figure S4C), indicating the IMNs (EpCAM & EGFR) can enhance the capture of mixed tumor cells more efficiently than IMNs (EpCAM) and IMNs (EGFR).

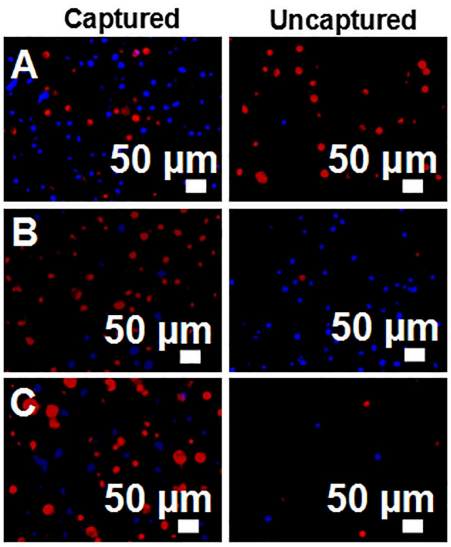

Figure S4. Fluorescence microscopic images of mixed MCF-7 cells (blue) and MDA-MB-231 cells (Red) treated with IMNs (EpCAM) (A), IMNs (CD45) (B) and IMNs (EpCAM & EGFR) (C). MCF-7 cells were Hoechst 33342-prestained and the MDA-MB-231 cells were DiI-prestained.

Optimization of IMNs (CD45) concentration and incubation time. The concentration of IMNs (CD45) and incubation time were optimized to achieve the best performance for white blood cells (WBCs) depletion with two consecutive rounds. In the first round, 5 x 10^6 Jurkat T cells were treated with different concentrations of IMNs (CD45) in 1 mL 1 x PBS for 30 min with continuous shaking at room temperature (RT), and they were also treated

with IMNs (CD45) in 1 mL 1 x PBS at different incubation time with continuous shaking at RT. Then, separated with a magnetic scaffold, the depleted and undepleted cells with IMNs (CD45) were all counted with a hemocytometer to calculate the depletion efficiencies. In the second round, we did the similar experiments to optimize the IMNs (CD45) concentration and incubation time in 800 μl 1 x PBS with 5 x 10^5 Jurkat T cells. The results were shown in Figure S4, in the first round, the depletion efficiency reached up to 87.8% with the IMNs (CD45) of 0.3 mg mL^{-1} (Figure S5A) and Figure S5B showed that the IMNs (CD45) (0.3 mg mL^{-1}) could efficiently deplete Jurkat T cells just within 15 min. Similarly, the depletion efficiency reached up to 91.6% with IMNs (CD45) of 0.2 mg mL^{-1} (Figure S5C) and the IMNs (CD45) could efficiently deplete Jurkat T cells just within 15 min (Figure S5D) in the second round. Considering that the more round, the little increasement of depletion efficiency, and the more loss of tumor cells, we employed two rounds of WBCs depletion, and 0.3 mg IMNs (CD45) were added to the samples and incubated for 15 min in the first round, 0.16 mg IMNs (CD45) were added to the samples and incubated for 15 min in the second round for following experiments.

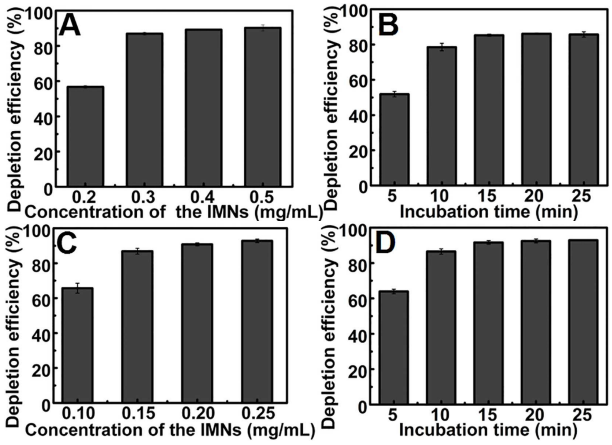

Figure S5. Efficiencies to deplete Jurkat T cells with different concentrations of IMNs (CD45) (A), and different incubation time (B) in the first round. Efficiencies to deplete Jurkat T cells with different concentrations of IMNs (CD45) (C), and different incubation time (D) in the second round.

Optimization of IMNs (EpCAM & EGFR) concentration and incubation time. The IMNs (EpCAM & EGFR) concentration and incubation time were optimized for achievement the best performance of capture tumor cells. The cocktail involved in 5 x 10^4 MCF-7 cells and 5 x 10^4 MDA-MB-231 cells was treated with different concentrations of IMNs (EpCAM & EGFR) in 400 μl 1 x PBS for 30 min with continuous shaking at RT, and they were also treated with IMNs (EpCAM & EGFR) in 400 μl 1 x PBS at different incubation time with continuous shaking at RT. Then, separated with a magnetic scaffold, the captured and uncaptured cells with IMNs (EpCAM & EGFR) were all counted with a hemocytometer to calculate the capture efficiencies. The results were shown in Figure S6, the capture efficiency increased with the increasing IMNs (EpCAM & EGFR) concentration, then reached a plateau of 93.1% when the IMNs (EpCAM & EGFR) concentration was higher than 0.3 mg mL^{-1} (Figure S6A). Besides, the capture efficiency with IMNs (EpCAM & EGFR) (0.3 mg mL^{-1}) reached up to 92.6% just within 15 min (Figure S6B). So the 0.12 mg IMNs (EpCAM & EGFR) were added to the samples and incubated for 15 min for following experiments..

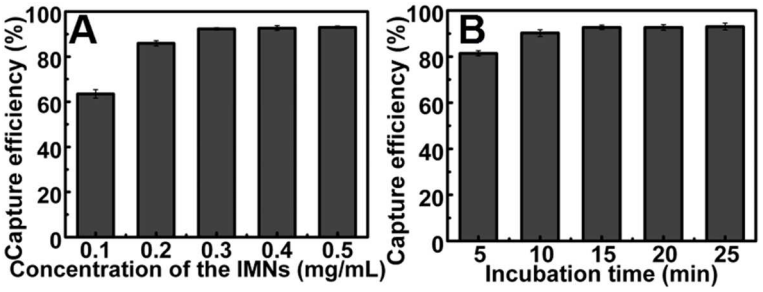

Figure S6. Efficiencies to capture tumor cells with different concentrations of IMNs (EpCAM & EGFR) (A), and different incubation time (B).

Table S1. Quantification of the trapped WBCs non-specifically among the enriched rare tumor cells in mimic clinical blood samples

Sample No.	1	2	3	4	5
Number of WBCs in 1 mL blood sample/1 x 10^6	6.08	8.23	7.63	7.02	4.04
Spiked number of tumor cells	15	55	92	141	227
Number of trapped WBCs non-specifically	1398	2052	1151	1809	1024
WBCs depletion efficiency/%	99.98	99.98	99.99	99.97	99.97

Table S2. Quantification of detected CTCs of blood samples from cancer patients

Sample No.	Cancer Type	Gender	Age	Volume processed/mL	CTCs
1	Liver	M	76	1	2
2	Liver	F	53	1	7
3	Liver	M	35	1	10
4	Liver	F	47	1	5
5	Liver	M	50	1	36
6	Breast	F	54	1	3
7	Breast	F	62	1	41
8	Breast	F	41	1	18
9	Breast	F	55	1	15
10	Colon	M	57	1	6
11	Colon	M	60	1	11
12	Colon	F	46	1	27

Table S3. Quantification of detected CTCs of blood samples from healthy people

Sample No.	Gender	Age	Volume processed/mL	CTCs
1	F	40	1	0
2	F	52	1	0
3	M	34	1	0
4	M	34	1	0